ANL-6434

Idaho

ANL-6434

Argonne National Laboratory

ELECTRICAL MEASUREMENTS ON THE GROWING SCALE ON ZIRCONIUM-TITANIUM ALLOYS

by

R. D. Misch and G. W. Iseler

LEGAL NOTICE

This report was prepared as an account of Government sponsored work. Neither the United States, nor the Commission, nor any person acting on behalf of the Commission:

A. Makes any warranty or representation, expressed or implied, with respect to the accuracy, completeness, or usefulness of the information contained in this report, or that the use of any information, apparatus, method, or process disclosed in this report may not infringe privately owned rights; or

B. Assumes any liabilities with respect to the use of, or for damages resulting from the use of any information, apparatus, method, or process disclosed in this report.

As used in the above, "person acting on behalf of the Commission" includes any employee or contractor of the Commission, or employee of such contractor, to the extent that such employee or contractor of the Commission, or employee of such contractor prepares, disseminates, or provides access to, any information pursuant to his employment or contract with the Commission, or his employment with such contractor.

ANL-6434
Metallurgy, Ceramics,
and Materials
(TID-4500, 16th Ed.,
Amended)
AEC Research and
Development Report

ARGONNE NATIONAL LABORATORY
9700 South Cass Avenue
Argonne, Illinois

ELECTRICAL MEASUREMENTS ON THE GROWING SCALE ON ZIRCONIUM-TITANIUM ALLOYS

by

R. D. Misch and G. W. Iseler

Metallurgy Division

Program 10.2.5

Work completed in 1960

Portions of the material in this report have appeared in the following Metallurgy Division Progress reports:

ANL-5975 pgs. 105-107

October 1961

Operated by The University of Chicago
under
Contract W-31-109-eng-38

TABLE OF CONTENTS

		Page
ABSTRACT		5
I.	INTRODUCTION	6
	A. General	6
	B. The Metal and Oxide Systems	6
	C. Oxidation of Zirconium-Titanium Alloys	6
	D. Previous Investigations of the EMF of Growing Scales	7
II.	THEORETICAL CONSIDERATIONS	7
	A. Electrical Parameters in the Oxidation Process	7
	B. Theoretical EMF's for the Oxide Scales on Zirconium-Titanium Alloys	9
III.	SPECIMEN PREPARATION	10
IV.	RESULTS OF OXIDATION IN WATER AND DRY OXYGEN	10
V.	ELECTRICAL MEASUREMENTS USING PLATINUM AS THE INERT PROBE	14
VI.	ELECTRICAL MEASUREMENTS USING CONDUCTING OXIDES	16
	A. General	16
	B. Preparation of Mixed Oxides	16
	C. Experimental Considerations	16
	1. General	16
	2. Thermal EMF's	17
	3. Comparison of Different Powders	17
	4. Area of Contact	18
	5. Methods of Measuring Resistance	18
	D. Results	19
	1. General	19
	2. 3.75 a/o Ti alloy	20
	3. 15.0 a/o Ti alloy	22
	4. 50.0 a/o Ti alloy	23
VII.	DISCUSSION	23
VIII.	ACKNOWLEDGEMENTS	25
IX.	REFERENCES	26

LIST OF FIGURES

No.	Title	Page
1.	Analogue of the corrosion cell in the scaling process	8
2.	Weight gains of low-titanium zirconium alloys in water at 290°C	10
3.	Weight gains of low-titanium zirconium alloys after 3 hrs in 1 atm oxygen at 500°C	11
4.	Corrosion weight gains upon heating zirconium-titanium alloys for 3 hrs in dry oxygen at the temperatures indicated	12
5.	Oxygen consumption curves for 3.75 a/o Ti and 50 a/o Ti zirconium alloys (1 atm O_2, 500°C)	13
6.	Oxygen consumption curves for 15 a/o Ti-zirconium alloys. Specimen Nos. 3 and 4 in 1 atm O_2, 500°C	13
7.	Curve of oxygen consumption for Specimen No. 1 (3.75 a/o Ti-zirconium alloy). (1 atm O_2, 500°C)	13
8.	Apparatus for measuring EMF and film resistance	17
9.	Variation of EMF and R during oxide growth on zirconium (1 atm O_2, 500°C)	19
10.	Changes of EMF of the growing oxide scale on specimens of 2.1 a/o Ti and 3.75 a/o Ti-Zr alloy in 1 atm oxygen at 500°C	20
11.	Changes of resistance of the growing oxide scale on specimens of 3.75 a/o Ti-Zr alloy in 1 atm oxygen at 500°C	21
12.	Changes of EMF of the growing oxide scale on specimens of 15 a/o Ti-Zr alloy in 1 atm oxygen at 500°C	21
13.	Changes of resistance of the growing oxide scale on specimens of 15 a/o Ti-Zr alloy in 1 atm oxygen at 500°C	22
14.	Changes of resistance of the growing oxide scale on specimens of 50 a/o Ti-Zr alloy in 1 atm O_2, 500°C	22

LIST OF TABLES

No.	Title	Page
I.	E_0 for the Oxidation of Zirconium-Titanium Alloys in Oxygen at 1 Atm and 500°C	9
II.	Rate Data for the Oxidation of Zirconium-Titanium Alloys in Oxygen at 1 Atm and 500°C	14
III.	EMF across the Growing Scale on Zirconium-Titanium Alloys as Measured by a Platinum Probe (1 atm oxygen, 500°C)	15
IV.	Ionic Radii and Ionization Potentials for Titanium and Zirconium	24

ELECTRICAL MEASUREMENTS ON THE GROWING SCALE ON ZIRCONIUM-TITANIUM ALLOYS

by

R. D. Misch and G. W. Iseler

ABSTRACT

The corrosion rates of low-titanium zirconium alloys increase with titanium content when exposed to water at 290°C or to 1-atm oxygen at 290, 350, 400, and 500°C. The scaling rate reaches a maximum (approximately 3000 mg/dm^2 for 3-hr exposure) at 15 a/o Ti in 1-atm oxygen at 500°C and then decreases with increasing titanium content. Under the same conditions, pure zirconium and titanium had much lower weight gains, 10 and 4 mg/dm^2, respectively.

In oxygen at 500°C, the oxidation rate law is initially cubic or parabolic for alloys containing 3.75, 15.0, and 50.0 a/o Ti, and then changes to approximately a linear one. The transition times are 17, 7, and 54 min for the 3.75, 15.0, and 50.0 a/o Ti alloys, respectively.

Transition in the rate law and the rise in EMF and resistance appear to be independent variables. The electrical changes are attributed to changes in defect structure, and the rate law transitions are attributed to structural changes.

The results provide an explanation for the maximum oxidation rate at 15 a/o Ti and for the differences in the influence of additives on the corrosion rates of zirconium and titanium in high temperature water.

The EMF of the corrosion cell consisting of [alloy | oxide | O_2] was a function of the resistance of the oxide layer. The 3.75 and 15.0 a/o Ti alloys had small EMF's and resistances initially, but EMF and resistance increased appreciably and rapidly at times after the transition stage. The 50 a/o Ti alloy had a very small EMF which was relatively constant while the resistance showed a slight increase with time.

I. INTRODUCTION

A. General

The corrosion of zirconium in water above 300°C is accelerated by the presence in the metal of certain elements, notably nitrogen, carbon, aluminum, and titanium.[1,2] Among the deleterious elements, titanium is of particular interest because of its close chemical similarity to zirconium. A titanium content of 100 ppm is sufficient to produce a deterioration in corrosion resistance. For this reason, zirconium-titanium alloys were selected for detailed study. The purpose of this investigation was to determine whether electrical changes in the mixed oxide film can explain the effect of titanium on the oxidation rate of zirconium.

B. The Metal and Oxide Systems

Titanium and zirconium metals are completely soluble with a minimum in the α-β transition temperature reported at 50 a/o Ti and 525°C.[3] At 650°C, where Hayes[4] studied the scaling rate, the alloy changed from α to β in the range from 25 to 35 a/o Ti.

The oxides ZrO_2 and TiO_2 are probably sufficiently soluble so that the film on low-titanium zirconium alloys will be a solid solution. Ksendzov and Prokhvatilov[5] found a maximum solubility of 10 mol % TiO_2 at 1400°C. In addition, a cubic $TiZrO_4$ phase was found. Brown and Duwez[6] indicated that the tetragonal form of ZrO_2 was favored by adding TiO_2. The solid solution range extended to 40 mol % TiO_2. In monoclinic ZrO_2 the solid solubility extended to approximately 5 mol % TiO_2. Wallaeys and Chaudron[7] showed good agreement with these results in the temperature range 600-1050°C.

C. Oxidation of Zirconium-Titanium Alloys

The effect of 2 to 12 w/o and 20 w/o titanium on zirconium oxidation was studied by Korobkov,[2] who stated that the worsening of the protective properties of the oxide film with an increase in the number of the ions of dissolved titanium appeared to be associated with an increase in the number of anion vacancies in the lattice of the oxide. This was based on the assumption that the titanium ions had a lower valence than Zr^{4+}. A slight decrease in the rate of oxidation with titanium additions above 8% was attributed to the precipitation of a second phase in the oxide film in the form of TiO_2.

At 650°C Hayes[4] found that the resistance to scaling became worse as the 50 a/o Ti composition was approached. This result was attributed to the fact that the 50 a/o alloy was in the faster-scaling β phase region.

D. Previous Investigations of the EMF of Growing Scales

Previous investigators used platinum to measure the EMF of growing scales. Kirkbride and Thomas[8] measured the EMF on zirconium in dry O_2 from 400 to 800°C and found that the EMF rose with temperature, reaching a maximum close to 1.3 volt at approximately 600°C. The EMF became erratic when water vapor was introduced into the system. Various other metals were studied by Dravnieks[9] and Hirschberg and Lange.[10]

In the case of cation-conducting scales in which the zone of scale growth is the scale-gas interface, it was desirable to avoid incorporation of the probe into the surface. In the case of zirconium and titanium for which the zone of scale growth is the metal-oxide interface, precautions should not be necessary.

II. THEORETICAL CONSIDERATIONS

A. Electrical Parameters in the Oxidation Process

Wagner[11] demonstrated the electrochemical nature of the scaling process and showed that the corrosion product is an electrolyte with conduction of both ions and electrons. The anodic process takes place at the metal-scale interface and the cathodic process at the scale-gas interface. Hoar and Price[12] presented a simplified model of the oxidation cell with separate ionic and electronic resistances.

In the oxidation of zirconium, the half-cell reactions are:

Anode: $Zr \rightarrow Zr^{4+} + 4e$

Cathode: $O_2 + 4e \rightarrow 2O^{=}$.

The electrons diffuse outward and the oxygen ions inward. The resulting cell will have a maximum EMF determined by the free energy of the total reaction

$$Zr + O_2 \rightarrow ZrO_2 \quad .$$

The theoretical or reversible EMF (denoted as E_0) will be distributed among the various steps in the oxidation process. These steps include the resistances in the oxide (both ionic and electronic) and the processes taking place at the interfaces. The interfacial processes, which involve electron transfer and diffusion of the reactants, will introduce activation potentials (overvoltage) or concentration changes (polarization). Polarization is characterized by the formation of a back EMF.

These steps in the oxidation process are shown in Figure 1, in which E_a and E_c represent the overvoltage and polarization contributions, and are shown at the interfaces, opposite in sign to E_0. By adding the separate terms, one obtains:

$$E_0 = iR_e + E_a + iR_i + E_c$$

or

$$E_0 = i(R_e + R_i) + E_a + E_c \quad ,$$

where E_0 is the reversible EMF for the reaction, i is the oxidation current, R_e and R_i are the electronic and ionic resistance, respectively, and E_a and E_c are the overvoltage and polarization contributions of the anode and cathode, respectively.

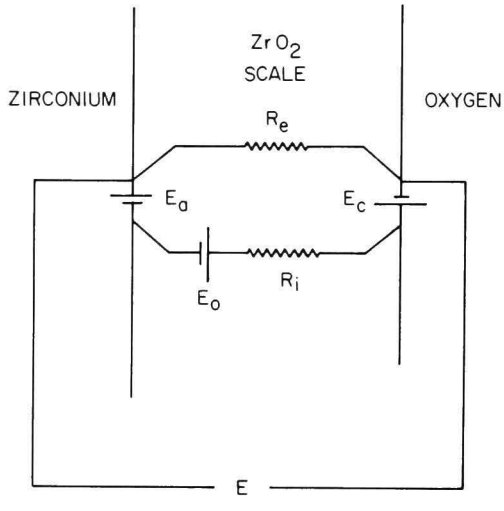

Fig. 1

Analogue of the corrosion cell in the scaling process.

If E_a and E_c are small relative to the IR drops, then

$$E_0 = i(R_i + R_e) \quad ,$$

where $iR_e = E$, the measurable EMF of the cell. Consequently

$$E_0 = iR_i + E$$

or

$$E_0 - E = iR_i \quad .$$

It is obvious that i goes to zero as E approaches E_0. The case of $E = E_0$ corresponds to zero electronic conductivity. From these expressions one may derive the ratio

$$\frac{E}{E_0} = \frac{R_e}{R_i + R_e} \quad .$$

This relation is identical to that derived by Wagner,[11] viz.,

$$E/E_0 = T_c + T_a = (1 - T_e) \quad ,$$

where T_c, T_a, and T_e are the cation, anion, and electron transference numbers, respectively.

If a direct measure of resistance is made, then the ionic and electronic resistances will act in parallel and

$$R_m = \frac{R_i R_e}{R_i + R_e} \quad .$$

In theory, one may calculate the corrosion current if E and R_m are available:

$$i = \frac{E_0 - E}{R_i} = \frac{E\,(E_0 - E)}{E_0 R_m} \quad .$$

If E is very small, i.e., the film is a good electronic conductor, this equation becomes

$$i = E/R_m \quad .$$

B. Theoretical EMF's for the Oxide Scales on Zirconium-Titanium Alloys

The theoretical EMF's for the formation of ZrO_2 and TiO_2 from the elements at 500°C and 1 atm are 2.56 and 2.00 volts, respectively. These values were calculated from data given by Kubaschewski.[13] If the EMF of formation of the dioxides from the alloys is assumed to be proportional to the mol fractions of the alloy constituents, the values given in Table I are obtained.

Table I

E_0 FOR THE OXIDATION OF ZIRCONIUM-TITANIUM ALLOYS IN OXYGEN AT 1 ATM AND 500°C

Atomic % Titanium	E_0 of Formation of the Dioxides, volt
0	2.56
3.75	2.54
15	2.48
50	2.28
100	2.00

III. SPECIMEN PREPARATION

Titanium and zirconium were obtained as iodide crystal bar. The titanium (A. D. Mackay, New York City) was stated to be 99.99% Ti. The zirconium was reactor grade (low hafnium) with the following spectrographic analysis: As, Ba, Ca, P, Sr, and Zn less than 0.1%; other elements less than 0.01%. Alloys were prepared by arc-melting three times in a water-cooled copper mold in a helium-argon atmosphere. The nominal and analyzed compositions were within the limits of error of the analyses. Consequently, losses during melting were negligible.

The specimens were machined into discs and were etched to a bright finish in 5 ml 47% HF, 45 ml 70% HNO_3, and 50 ml distilled water.

IV. RESULTS OF OXIDATION IN WATER AND DRY OXYGEN

Corrosion rates in water were determined by the increase in weight caused by the formation of the oxide scale. Specimens were exposed to degassed distilled water at 290°C in a static autoclave. The water was replaced whenever the autoclave was opened to weigh the specimens. Titanium increased the corrosion rate of zirconium in 290°C water, as shown in Figure 2. When the weight gains exceeded 20 mg/dm^2, the initially black oxide film began to turn grey and finally white.

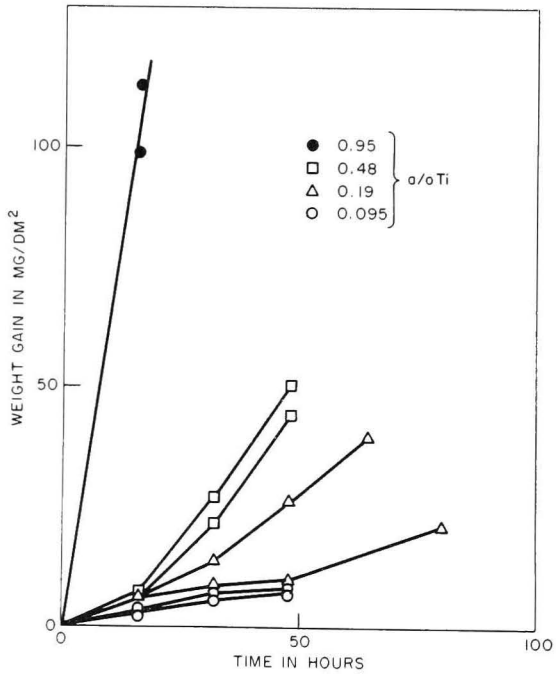

Fig. 2

Weight gains of low-titanium zirconium alloys in water at 290°C.

The scaling rate in oxygen was measured either by weight gain or by oxygen consumption. The former method was used to determine the oxidation behavior for the entire Zr-Ti system. A series of alloys were exposed to oxygen at 1 atm at 290, 350, 400 and 500°C for 3 hr. Commercial tank oxygen was used after drying over Molecular Sieve,* a desiccant for which high efficiency has been claimed.(14) Weight-gain data for the low-titanium alloys are shown in Figure 3; data for the entire binary system are shown in Figure 4. After oxidation, the appearances of the specimens varied, depending on their weight gain. Extreme cases are represented by pure zirconium which had an adherent, nearly black, coating and 15 a/o Ti which had a cream-colored layer which had flaked along the edges. This layer appeared translucent when viewed microscopically.

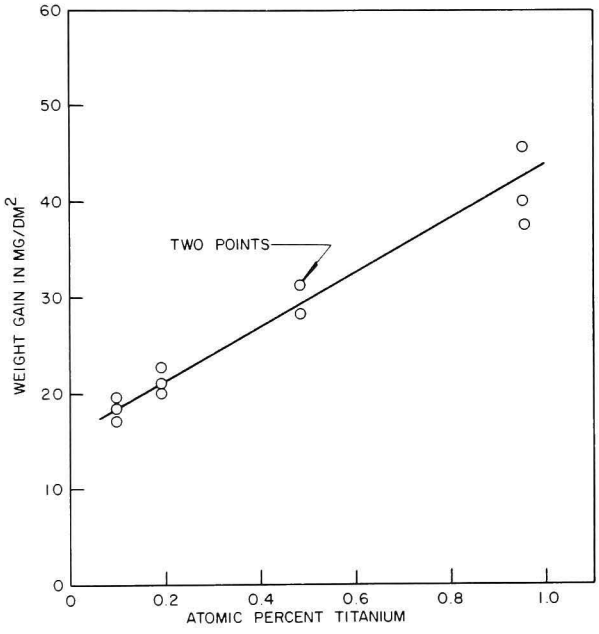

Fig. 3

Weight gains of low-titanium zirconium alloys after 3 hr in 1 atm O_2 at 500°C.

All specimens with weight gains exceeding 1000 mg/dm^2 were similar to the 15 a/o Ti alloy. In some cases the change from black to white oxide was incomplete, and the surface had patches of white oxide. The thicknesses of the heavy oxide layers were found to exceed the thicknesses calculated from an assumption of dense oxide. This was taken as an indication of porosity in these layers. The 50 a/o Ti specimen was dull black without the luster of the film on pure zirconium. The higher titanium alloys were black with some iridescence.

*Linde Company, Tonawanda, New York.

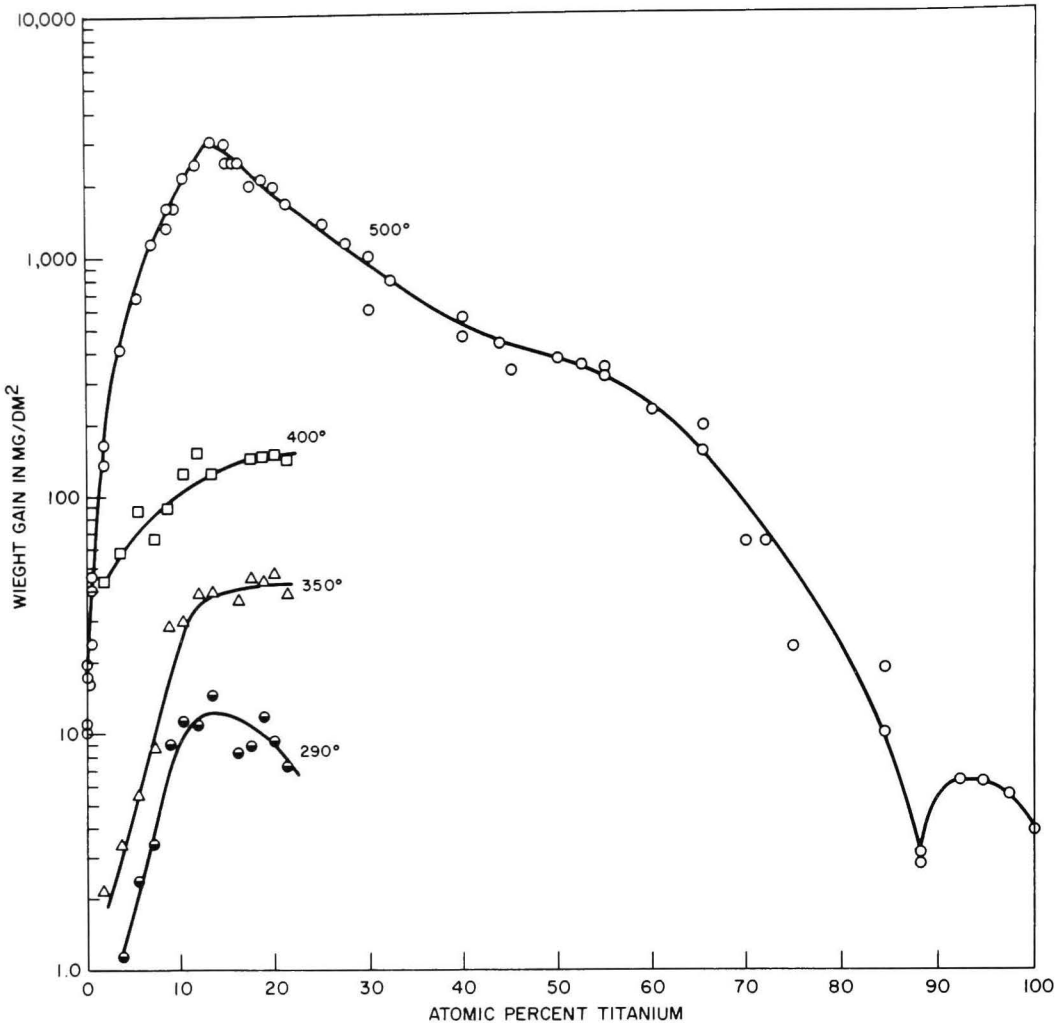

Fig. 4

Corrosion weight gains upon heating titanium-zirconium alloys for 3 hr in dry oxygen at the temperatures indicated.

Three alloys were examined in greater detail. These were 3.75 and 50 a/o Ti, which had approximately equal weight gains after three hours, and also 15 a/o Ti, which had the maximum weight gain. The oxidation rates for these three alloys were determined in a volumetric apparatus which measured the oxygen consumed at constant pressure. This work was performed by Howard A. Porte and J. G. Schnizlein of the Chemical Engineering Division. The apparatus has been described in a previous report.(15)

The reactor enclosing the specimens was evacuated at room temperature for 16 hr at pressures of less than 10^{-5} mm Hg to minimize outgassing when the system was brought to temperature. The specimens were then heated in vacuum, and oxygen at 760 mm Hg pressure was admitted soon after thermal equilibrium was established. Both specimens were oxidized for 400 min.

The results are presented in Figures 5 and 6, in which each curve represents a separate specimen. Except for the initial period the curves are approximately linear, a designation is used in the absence of any other well-defined relationship. The rate law behavior became clearer when the data (including points not shown on Figures 5 and 6) were plotted on log-log paper. An example of such a plot is given in Figure 7 for specimen 1 of Figure 5.

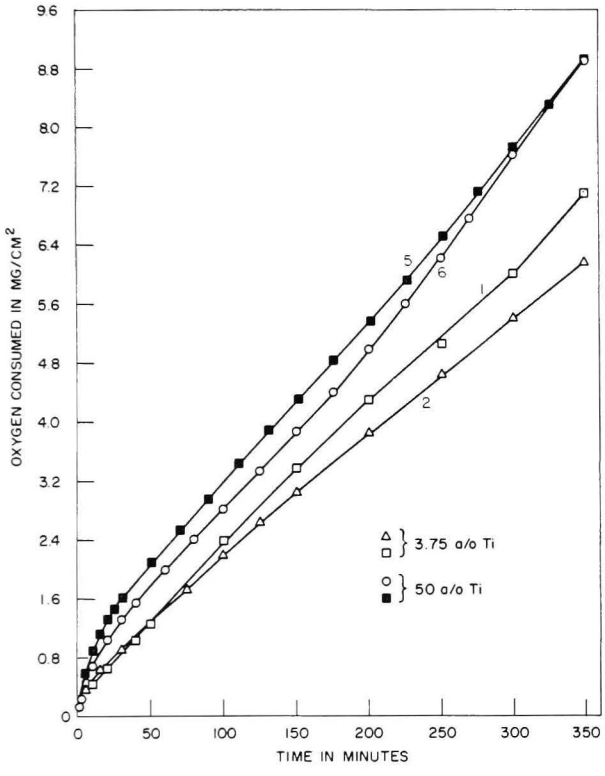

Fig. 5

Oxygen consumption curves for 3.75 a/o Ti and 50 a/o Ti zirconium alloys (1 atm O_2, 500°C).

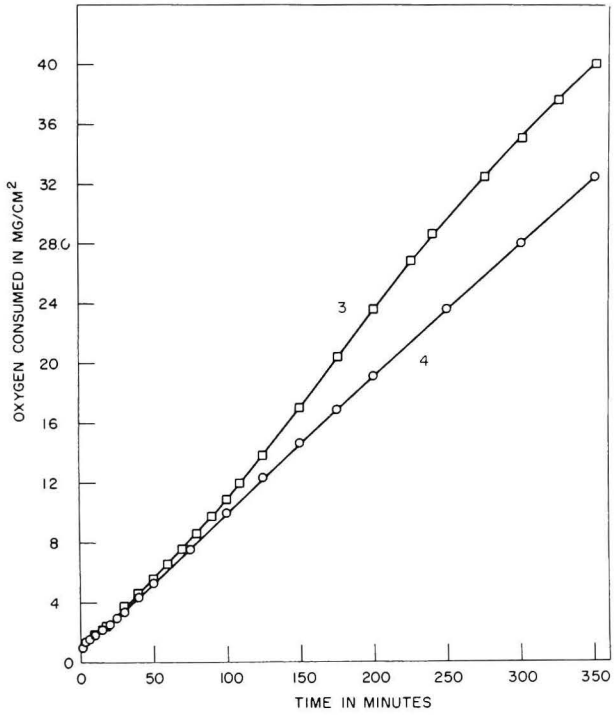

Fig. 6

Oxygen consumption curves for 15 a/o Ti-zirconium alloys. Specimen Nos. 3 and 4 in 1 atm. O_2, 500°C.

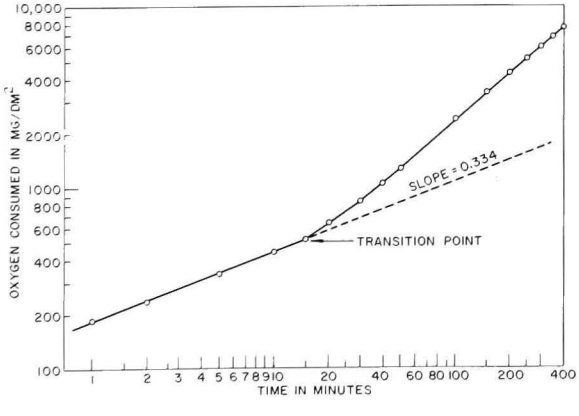

Fig. 7

Curve of oxygen consumption for specimen No. 1 (3.75 a/o Ti-zirconium alloy) (1 atm O_2, 500°C).

This plot shows a well-defined transition between two periods of different slope. The data from such plots are summarized in Table II, in which the transition times and the weight and pre- and post-transition rates are given.

Table II

RATE DATA FOR THE OXIDATION OF ZIRCONIUM TITANIUM ALLOYS IN OXYGEN AT 1 ATM AND 500°C*

Sample No.	Atom Per cent Titanium	Pre-breakaway Slope, 1/N	Break-away Time, min	Break-away Weight, mg/dm^2	Break-away Thickness, microns	Linear Rate, mg/dm^2/min	Oxygen Consumed after 400 min, mg/dm^2	Oxide Thick-ness after 400 min, microns	Appearance after Exper-iment
1	3.75	0.33	15	54.0	3.32	1.93	763.8	47.0	Light gray, adherent oxide
2	3.75	0.45	20	72.3	4.46	1.67	691.8	42.5	Light gray, adherent oxide
3	15.0	0.27	7.5	180.0	11.1	11.8	4461	274	Beige-colored adherent oxide
4	15.0	0.21	6.0	154.5	9.50	9.05	3673	226	Beige-colored adherent oxide
5	50.0	0.51	52	210.0	12.9	2.28	1019	62.7	Very flaky beige oxide
6	50.0	0.61	56	188.0	11.6	2.24	1024	63.0	Very flaky beige oxide

*Data from ANL-RCV-SL-1389, September 3, 1958, Argonne Chemical Engineering Division.

The 3.75 and 15.0 a/o Ti alloys can be said to follow a cubic law prior to transition, because their slopes were close to $\frac{1}{3}$ or 0.33. The 50.0 a/o Ti alloy can be said to follow a parabolic law before transition, for the slope was close to $\frac{1}{2}$ or 0.50. As expected, the 15 a/o Ti alloy had the shortest transition times and the highest rates after transition.

V. ELECTRICAL MEASUREMENTS USING PLATINUM AS THE INERT PROBE

A preliminary study of EMF was made by using a platinum probe which touched the surface of the oxide. The probe was made from 0.010-in.-diameter wire with a rounded tip prepared by fusing in a flame. The zirconium under the scale formed the second contact. Estimates of the contact area from measurements of constriction resistance were of the order of 10^{-6} cm^2.(16)

In most cases when zirconium was oxidized with such a probe on the surface, an EMF appeared within several minutes after reaching 500°C and rose to a peak of 1.0 to 1.2 V within 10 to 40 min. In other cases the EMF did not rise above 0.2 V within 10 to 40 min. A range of EMF and resistance was measured when the probe was moved from one point to another on the surface. An EMF was always associated with resistance of the oxide under the probe.

The probe method was applied to a number of alloys which were oxidized for a 3-hr period. The results are given in Table III, in which the EMF range and most typical EMF are given. EMF readings of zero were disregarded for the reason that mechanical damage to the film produced a drop in EMF. The probe was moved every three minutes. Resistance was also measured, but the variation was so great that meaningful values could not be given. Most of the observed EMF's were close to the "most typical EMF" instead of to an arithmetic average which would be misleading. The EMF first appeared after an induction period which was 20 to 30 min for zirconium and less for the alloys. The EMF was obviously a maximum on pure zirconium and dropped with titanium content.

Table III

EMF ACROSS THE GROWING SCALE ON ZIRCONIUM-TITANIUM ALLOYS AS MEASURED BY A PLATINUM PROBE

(All measurements were taken in oxygen at 1 atm and 500°C over a 3-hr period, except as noted. The probe was placed on a new area every 3 min.)

Titanium Content, a/o	EMF Range, volt	Most Typical EMF, volt
0	0.5 to 1.5	1.25
1.9	0.1 to 0.9	0.4
3.75	0.2 to 0.55	0.3
5.6	0.15 to 0.43	0.25
7.3	0.1 to 0.4	0.25
12.5*	~0.4	0.4
14.2*	0.2 to 0.4	0.3
19.0	0.2 to 0.35	0.28
20.6	0.1 to 0.2	0.15
22.1	0.05 to 0.125	0.11
23.7	0.05 to 0.125	0.06

*1-hr experiment.

Following this experiment, an attempt was made to use a number of probes simultaneously and to average the data. This method failed because of electrical leakage among the probes. Because of the high impedance of the electrometer it was not possible to reduce this leakage to a point where the effect on the measurements became negligible. A third method of contacting the surface with platinum was to use platinum black confined to a known area by a platinum ring. The EMF was not stable, and the powder was found to sinter at 500°C, so that the area of contact could not be assumed constant. Substitution of a gold probe for platinum gave the same results and did not improve the stability.

VI. ELECTRICAL MEASUREMENTS USING CONDUCTING OXIDES

A. General

After experiencing difficulties with platinum, another contact material was desired which was electronically conducting and stable in oxygen over a range of temperatures. Free access of oxygen to the metal scale was also necessary. After choosing oxides as the most promising contact material, the review by Meyer[17] provided a survey of the conductivities of oxides. However, none of these promised to be satisfactory. The reason was that the most highly conducting oxides were the lower valence forms, such as FeO and MnO. In the presence of oxygen these lower oxides would tend to form the poorly conducting higher oxides. Other causes of rejection were low melting point and volatility.

When nickel oxide was tested in preliminary work, it was found that a very stable EMF could be measured in oxygen. However, the pure oxide had a rather high resistance and was not suitable for measuring film resistance.

B. Preparation of Mixed Oxides

To circumvent this difficulty, a mixed oxide was used in which conductivity was promoted by valency control. Two promising oxide combinations were investigated: Fe_2O_3 containing TiO_2, and NiO containing Li_2O. The mixed oxides may be represented by the formulas $Ti_{0.1}Fe_{1.9}O_3$ and $Li_{0.1}Ni_{0.9}O$. The $Ti_{0.1}Fe_{1.9}O_3$ was prepared by the method of Déri[18] and the $Li_{0.1}Ni_{0.9}O$ was prepared by the method of Verwey.[19] The substitution of Ti^{4+} for Fe^{3+} produced a good n-conductor and the substitution of Li^{+} for Ni^{2+} produced a good p-conductor. After pressed pellets of the mixed oxides were sintered, they were crushed and sieved to -100 +150. This size range was chosen because finer particles had poorer conductivity while large particles were only slightly higher in conductivity. A small particle size was desired to ensure as many points of contact as possible.

C. Experimental Considerations

1. General

The powder was used by placing it in a cone-shaped depression in a platinum support. The experimental arrangement is illustrated in Figure 8. The zirconium alloys were machined into $\frac{1}{4}$-in.-diameter rod with a 120° cone-shaped tip. By this means the specimen tended to center itself in the platinum support, and thermal EMF's due to temperature gradients were reduced to a minimum.

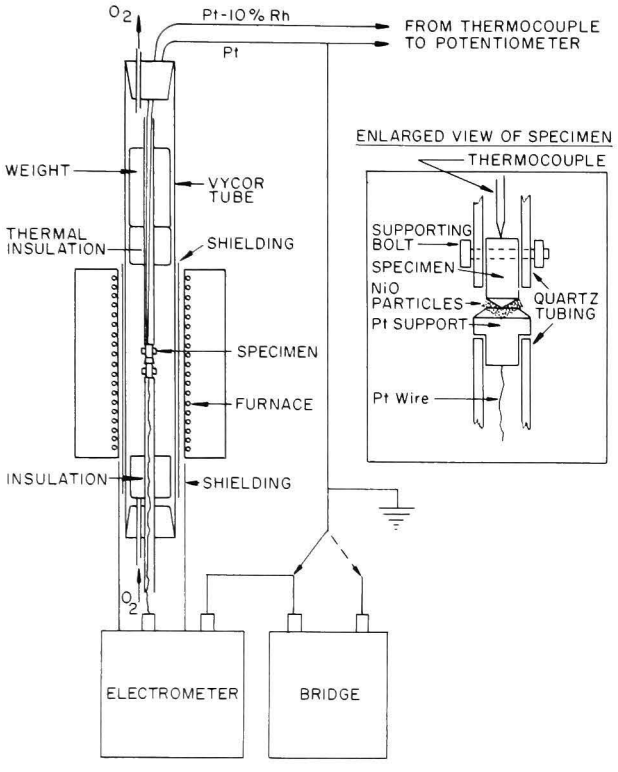

Fig. 8

Apparatus for measuring EMF and film resistance

In all experiments the specimen was loaded with a total weight of 500 gm (1.6 kg/cm^2). Without the application of pressure, the resistance of the powder rose by a factor of 10 or more and varied erratically during an experiment. With pressure, the resistance of the powder was low and uniform. Prior to heating, the system was flushed with oxygen. The gas flow was then reduced to about 1 ml/sec, and heating was started. During an actual measurement the specimen was brought to 500 ± 2°C in 7 to 8 min, and EMF and resistance were measured as often as convenient.

2. Thermal EMF's

The Zr-Pt thermal EMF is less than 15 mv at 500°C[20] and, therefore, made no important contribution to the measured EMF. However, some initial difficulty was experienced with the oxide powders which have high thermal EMF's and are sensitive to temperature gradients in the system. Such EMF's were especially noticeable during the heating period. As a result of redesign of the system, the thermal EMF was reduced to 1 mv under the conditions used during measurement.

3. Comparison of Different Powders

The resistance of the $Ti_{0.1}Fe_{1.9}O_3$ powder in a typical run averaged 250 ohms initially at room temperature and dropped to 10 ohms at 500°C. Upon cooling to room temperature the resistance had risen to several thousand ohms. Each reheating produced an increase in resistance at room temperature. This resistance increase was attributed to formation of a high-resistance layer on the surface in the presence of oxygen. By contrast, a p-type oxide, such as $Li_{0.1}Ni_{0.9}O$, should not form a high-resistance layer. This prediction was borne out when the resistance of the $Li_{0.1}Ni_{0.9}O$ did not change appreciably after several heating cycles. The initial resistance of this oxide was 150 ohms at room temperature and 3 ohms at 500°C.

The same corrosion EMF's were obtained using either powder, and it was decided to use only $Li_{0.1}Ni_{0.9}O$. A mixed oxide of similar composition, $Li_{0.05}Ni_{0.95}O$, has been studied for thermoelectric applications and was found by Danko to lose very little lithium after 1200 hr at 900°C.[21] The same report indicated that no reaction took place between $Li_{0.05}Ni_{0.95}O$ and ZrO_2 after 24 hr at temperature up to 1100°C.

4. Area of Contact

Various attempts were made to determine the area of contact of the oxide powder with the growing scale, but no method was found which gave satisfactory results. In addition, it would be necessary to assume that current flow through the scale would be normal to the surface during the time in which the scale was thickening. In the absence of reliable corrosion product resistivities it was not possible to calculate corrosion currents.

5. Methods of Measuring Resistance

Either ac or dc could be employed to measure resistance. In the ac method a bridge imposed 30 mv at 1 kc across the oxide scale. In the dc method a series of known resistances were shunted in across the electrometer, and the scale resistance was calculated from the IR drop. The ac and dc methods agreed within experimental error, but the ac method was preferred for several reasons. Among these were the following:

When the oxide resistance was high, the dc measurement required more time and the results were more variable than was the case when ac was used. When the scale resistance was low and the dc method was used, the drain on the corrosion cell in the scale produced a resistance increase in the corrosion film. This effect could be circumvented by applying a back EMF which lowered the net EMF to the order of 10 mv.

D. Results

1. General

When oxidizing zirconium and titanium at 500°C in oxygen at 1 atm for times up to 24 hr, an EMF appeared with zirconium but not with titanium. The resistance of the oxide could be measured for zirconium but remained negligible for titanium.

The EMF of the oxide on zirconium sometimes rose rapidly and sometimes slowly. Some erratic characteristics were always observed, which were associated with the thinness of the oxide film.

In a typical case, the EMF with pure zirconium was less than 0.3 mv for approximately 15 hr and then began to rise. Up to 15 hr the resistance rose from less than 1 ohm to 60 ohms. The EMF and resistance then rose more rapidly, but varied erratically for a period up to approximately 24 hr. In the erratic period, a high EMF was always accompanied by a high resistance. By taking numerous readings in this interval, a plot of E and R_m was made and is given in Figure 9. The slope of this curve is E/R_m where

$$E/R_m = E_0/R_i \quad .$$

Because $E_0 = 2.56$ v, $R_i = 1.35 \times 10^6$ ohms.

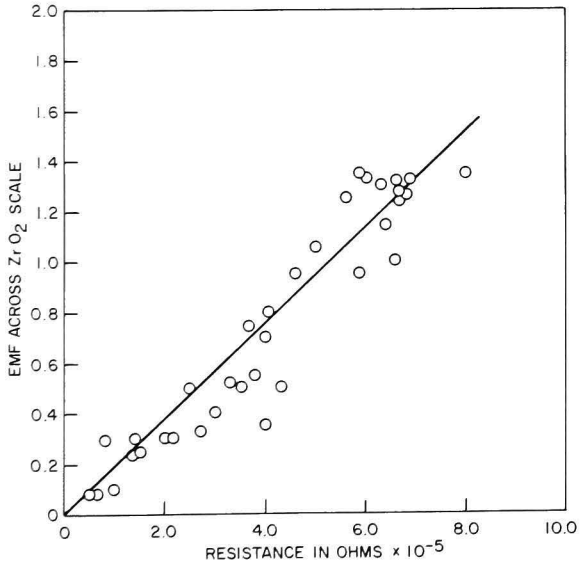

Fig. 9

Variation of EMF and R during oxide growth on zirconium (1 atm O_2, 500°C).

After the erratic period, both E and R_m remained high for approximately 32 hr. Then E decreased slowly to 0.85 v at the end of the experiment at 47 hr. After 24 hr, R was relatively constant at 6×10^5 to 7×10^5 ohms. The specimen had a uniform black film when the experiment was concluded.

In general, oxide growth on both titanium and zirconium was too slow at 500°C to make the pure metals suitable for study at this temperature. Oxide growth on the alloys was much more rapid, and changes in EMF and resistance were readily observed.

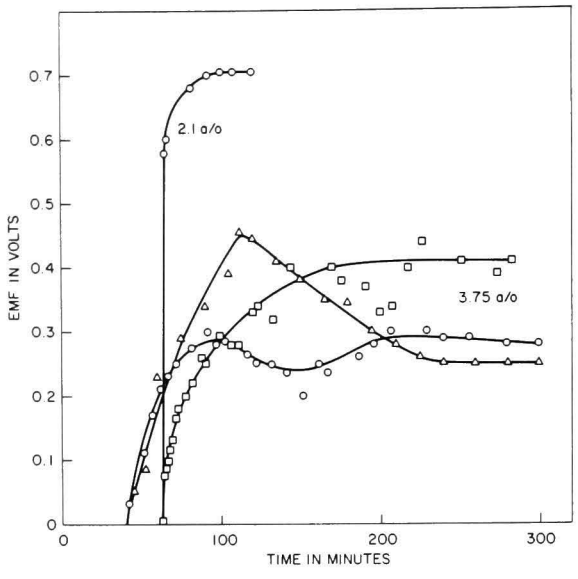

Fig. 10

Changes of EMF of the growing oxide scale on specimens of 2.1 a/o Ti and 3.75 a/o Ti-Zr alloys in 1 atm oxygen at 500°C. Three experiments are shown for the 3.75 a/o Ti alloys.

In the course of measurements on the 3.75 and 15.0 a/o Ti alloys, one of the original objectives of determining both EMF and resistance for the same specimen could not be realized. The larger changes in these variables were rapid, and switching from one measurement to another did not provide satisfactory results. Consequently, separate determinations were necessary. The data of Figures 10, 11, 12, 13 and 14 for EMF and resistance represent individual measurements.

2. 3.75 a/o Ti Alloy

The 3.75 a/o Ti alloy developed an EMF rapidly. The data are given in Figures 10 and 11. From Figure 10 it is apparent that the observed EMF's diminished as the concentration of titanium increased. A 2.1 a/o Ti alloy was included in Figure 10 for comparison. Whereas pure zirconium reached 1.3 v, the 2.1 a/o alloy reached 0.7 v and the 3.75 a/o alloys did not exceed 0.45 v. Comparison with Figure 11 indicates that a large increase in resistance accompanied the rapid increase in EMF. Below 10^2 ohms the EMF was no more than several millivolts. Above 10^2 ohms the resistance often increased in jumps and each jump was accompanied by an increase in EMF. The curves do not show these jumps well because the change in resistance covered a wide range and the resistance often rose and dropped erratically before stabilizing at the high resistance. This behavior was illustrated in Figure 9. As a consequence, stable readings were not easy to obtain in the region where the resistance rose rapidly. Direct observation indicated that the abrupt increase in resistance was usually by a factor of 10^2 to 10^3. Above 10^6 ohms the resistance increased more slowly, rising to a maximum between 10^7 and 10^8 ohms.

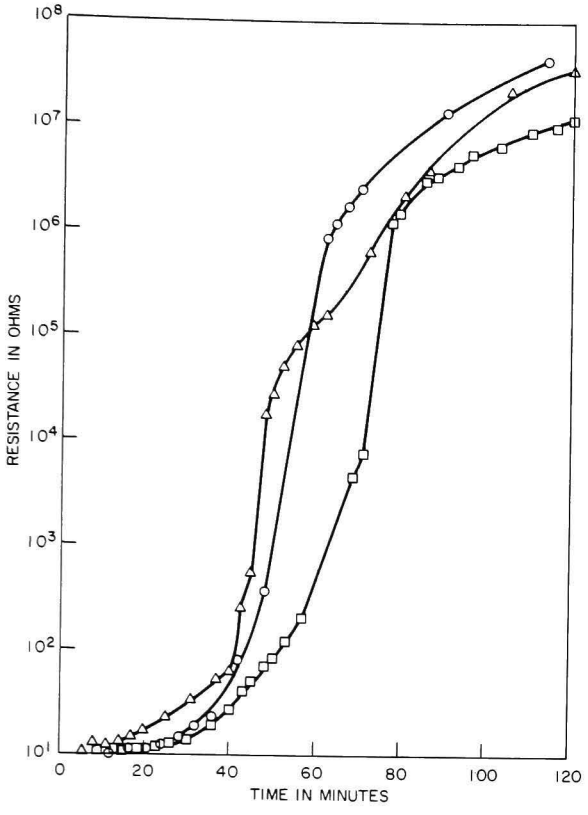

Fig. 11

Changes of resistance of the growing oxide scale on specimens of 3.75 a/o Ti-Zr alloy in 1 atm oxygen at 500°C

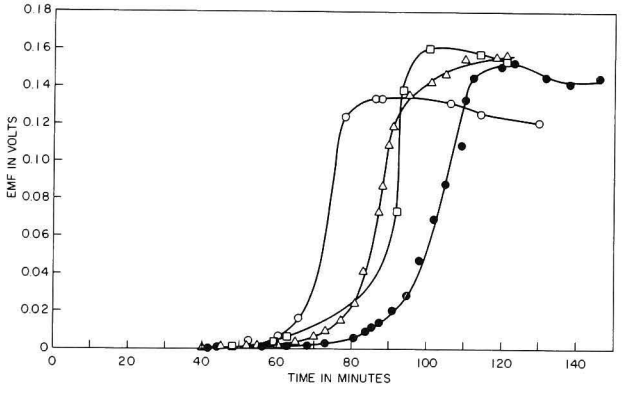

Fig. 12

Changes of EMF of the growing oxide scale on specimens of 15 a/o Ti-Zr alloy in 1 atm oxygen at 500°C

There were no changes in EMF and R which could be related to the change in rate law from cubic to linear at 15 min. The oxide was shiny black initially, but white oxide developed at scattered spots and grew until the entire specimen was white upon removal at 120 min. It is believed that the large increase in resistance coincided with the change from black to white oxide, because other specimens removed within the 40- to 80-min period were in various stages of transition. As seen in Figure 10, the EMF dropped in two cases after reaching a maximum. No reason for these changes could be determined.

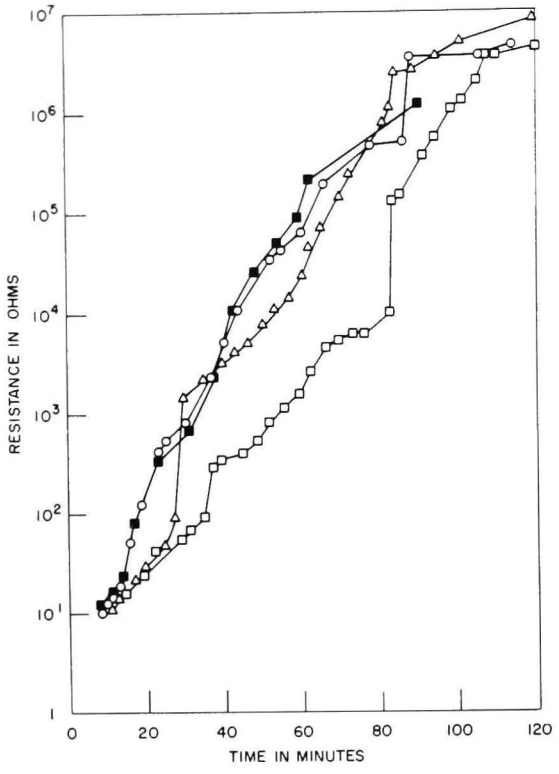

Fig. 13

Changes of resistance of the growing oxide scale on specimens of 15 a/o Ti-Zr alloy in 1 atm oxygen at 500°C.

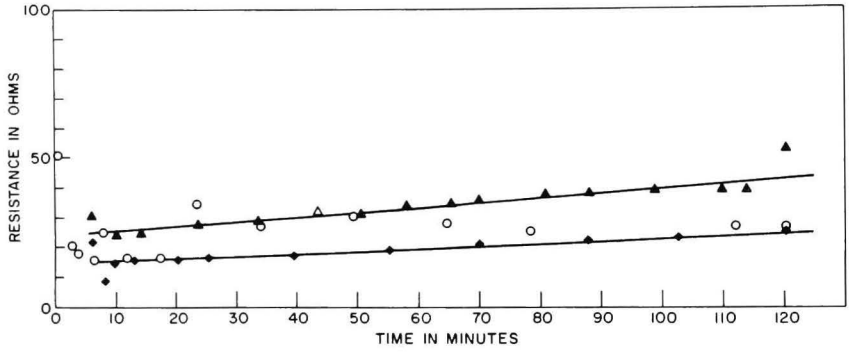

Fig. 14

Changes of resistance of the growing oxide scale on specimens of 50 a/o Ti-Zr alloy in 1 atm O_2, 500°C

3. 15.0 a/o Ti Alloy

The 15 a/o Ti alloy showed a slow increase of EMF, with the largest increase taking place between 70 and 100 min. The change in resistance was more uniform than in the case of the 3.75 a/o alloy. Jumps in resistance were still observed, but were usually not greater than a factor of 10. Erratic periods were almost completely absent. The breakaway time for this alloy was so short (cf. Table I) that it was not covered by the data for EMF and resistance. The maximum EMF (0.13 to 0.16 v)

was much less than for the 3.75 a/o alloy, indicating that the oxide was a better conductor at 500°C. The oxide scale was much thicker than the scale on the 3.75 a/o alloy after the same period of time. Specimens of the 15 a/o alloy were found to change from a shiny black to a cream color more rapidly than the 3.75 a/o alloy. Again the oxide is believed to have changed from black to white in the region of rapid rise in EMF.

4. 50.0 a/o Ti Alloy

In the case of the 50 a/o Ti-Zr alloy, the EMF during film growth was close to the limit of the thermal EMF. The EMF did not exceed 2-3 mv during three experiments conducted for 120 min. The resistance was 10-30 ohms initially and seemed to increase very slowly with time. The resistances are plotted in Figure 14. Assuming that the EMF was constant as well as small, the corrosion current would be expected to diminish very slowly with time.

The breakaway time (52-56 min) was conveniently observable, as seen from Table II, but no change in EMF or resistance was observed. The oxide remained dull black during the course of oxidation.

VII. DISCUSSION

On pure zirconium the oxide formed slowly and had a high resistance. The maximum EMF was approximately half of E_0. Consequently, R_i and R_e must have been of the same order of magnitude, as seen from the equation

$$\frac{R_i}{R_e} = \frac{E_0 - E}{E} \quad .$$

In the oxidation of pure titanium, R_e was very small and R_i must have been rate controlling.

In the case of the 3.75 a/o and 15 a/o Ti alloys the transition to a linear rate law did not influence the EMF and resistance. The sharp rise in EMF, accompanied by an increase in resistance, could have resulted from the same changes that gave rise to white oxide. On the 15 a/o Ti alloy the oxide formed rapidly and maintained a low resistance until the thickness was many times larger than on zirconium in the same period of time. Cracking then set in, and the film developed a high resistance.

In the case of the 50 a/o alloy, an increase in resistance at the transition point (after approximately 54 min) would have been easy to recognize. The EMF and resistance both remained low throughout this interval.

After transition the resistance must represent a composite of the resistances of two or more layers. This conclusion is based on the interpretation of the linear oxidation law as resulting from a barrier layer of constant thickness. It was also confirmed by work on the capacitance of oxide layers.[22]

Because the resistance did not reflect the transition, it must be concluded that the changes were not in the overall structure or stoichiometry of the oxide. A possible explanation is the formation of vertical cracks penetrating part of the way to the metal oxide interface. This cracked layer then changed further at the time when the rapid rise in EMF and resistance occurred. It is suggested that the stoichiometry of the outer layer is changing as a result of oxygen penetrating along the initial cracks. As the oxide thickens, the outer layer will break up more and more until the typical white oxide appears. These conclusions may not be applicable to the oxidation of other zirconium alloys where separate phases may appear in the oxide scale. The situation in such cases could become very complicated.

The change in EMF provides an explanation for the peak in oxidation rate at 15 a/o Ti. The substitution of titanium for zirconium in the ZrO_2 lattice is presumed to form Ti^{3+} ions which can participate in electron exchange and thereby enhance the electronic conductivity. The presence of Ti^{3+} will also form anion vacancies which will increase the ionic conductivity. Consequently, both R_e and R_i will diminish and the oxidation rate will rise. The drop in rate at higher titanium concentrations can be explained by structural changes, contraction of the ZrO_2 lattice, or the formation of increasing amounts of $TiZrO_4$. Korobkov[2] also suggested that Ti^{3+} explained the increased oxidation rate of Ti-Zr alloys. The ionic radii and ionization potentials of titanium and zirconium are favorable to this possibility, as shown in Table IV.

Table IV

IONIC RADII AND IONIZATION POTENTIALS FOR TITANIUM AND ZIRCONIUM

Element	Ionic radius[23] of M^{4+} (Å)	Ionization potential[24] (eV) $M^{3+} \rightarrow M^{4+} + e$
Ti	0.64-0.68	43.24
Zr	0.80-0.89	33.97

The smaller size of Ti^{4+} provides more room in the lattice to form the larger Ti^{3+}, and more energy is required to form Ti^{4+} than Zr^{4+}.

The effect of titanium upon the oxidation rate of zirconium in water is even greater than the effect in oxygen. Therefore, some explanation is required beyond the explanation for oxygen alone. The hydrogen damage mechanism of Draley and Ruther[25] may be the critical factor. It is also possible that the dissolution of hydrogen in the mixed ZrO_2-TiO_2 lattice may have specific effects. As shown by Heckelsberg,[26] the solution of hydrogen in n-conductors has the effect of increasing the electronic conductivity. P-conductors showed a decrease. In any case, the changes in conductivity of the oxide scale undoubtedly play an important role in the oxidation process.

VIII. ACKNOWLEDGEMENTS

The form of the equations for EMF and resistance was worked out in collaboration with J. E. Draley, whose advice and consultation is gratefully acknowledged. Appreciation is also due to J. G. Schnizlein and H. A. Porte, who determined the oxygen-consumption curves on their equipment. Analyses of the alloys to confirm their composition were made by members of the Chemistry Division.

REFERENCES

1. Chapter by D. E. Thomas, p. 608 in The Metallurgy of Zirconium, B. Lustman and F. Kerze, Jr., Eds., McGraw-Hill, New York (1955).

2. I. I. Korobkov et al., Electron Diffraction and Kinetic Investigations of the Oxidation Reactions of Zirconium and Some of Its Alloys, Proceedings of the Second United Nations Internationl Conference on the Peaceful Uses of Atomic Energy, United Nations, Geneva 5, 60, (1958).

3. M. Hansen and K. Anderko, Constitution of Binary Alloys, McGraw-Hill, New York (1958), p. 1245.

4. E. T. Hayes, A. H. Roberson and O. G. Paasche, Zirconium-Titanium System: Constitutional Diagram and Properties, Bur. Mines Rept. Invest. 4826 (Nov 1951).

5. Ya. M. Ksendzov and V. G. Prokhvatilov, Zhur. Fiz. Khimii, 31, 321-327 (1957).

6. H. F. Brown and P. Duwez, J. Am. Ceram. Soc., 37, 129-132 (1954).

7. R. Wallaeys and G. Chaudron. Colloq. nationaux centre natl. recherche sci. (Paris), No. 11, Chim. Hautes Temp. Paris, 1954, 155-61 (Pub. 1955).

8. L. D. Kirkbride and D. E. Thomas, Ionic Transport in Zirconium Oxide, WAPD-T-308.

9. A. Dravnieks and H. J. McDonald, Trans. Electrochem. Soc., 93, 177-190 (1948).

10. R. Hirschberg and E. Lange, Naturwissenschaften, 39, 187 (1952).

11. C. Wagner, Z. physik, Chem. (B) 21, 25 (1933).

12. T. P. Hoar and L. E. Price, Trans. Faraday Soc., 34, 867 (1938).

13. O. Kubaschewski and E. L. Evans, Metallurgical Thermochemistry, 3rd ed., Pergamon Press, New York (1958).

14. C. C. Addison, E. Iberson, and J. D. Raynor, Chemistry and Industry, 77, 96 (1858).

15. H. A. Porte, J. G. Schnizlein, R. C. Vogel, and D. F. Fischer, ANL-6046 (Sept 1959), p. 15; Also, J. Electrochem. Soc., 107, 506-515 (1960).

16. R. D. Misch and F. H. Gunzel, Jr., J. Electrochem. Soc., 106, 15-20 (1959).

17. W. Meyer, Z. Elektrochem. 50, 274-290 (1944).

18. M. Déri and J. Millner, Acta Chim. Acad. Sci. Hung., 5, 215-33 (1955).

19. E. J. W. Verwey, P. W. Haaijman, F. C. Romeijn, and G. W. van Oosterhout, Philips Res. Repts., 5, 173-187 (1950).

20. L. L. Wyman, KAPL-852 (Dec. 19, 1952).

21. Thermoelectric Nuclear Fuel Element Annual Progress Report, WCAP-1162, J. C. Danko, Director (April 15, 1959).

22. R. D. Misch, ANL-6149 (May 1960).

23. D. E. Gray, American Institute of Physics Handbook (1957).

24. C. E. Moore, Atomic Energy Levels, 1st ed., Washington, D. C. (1949, 1950).

25. J. E. Draley and W. E. Ruther, J. Electrochem. Soc. 104, 329-333 (1957).

26. L. F. Heckelsberg, G. C. Bailey, and A. Clark, J. Am. Chem. Soc. 77, 1373 (1955).

ARGONNE NATIONAL LAB WEST
3 4444 00011918 0